RESEARCH ARTICLE

Fuel Cells
FROM FUNDAMENTALS TO SYSTEMS

Development and full system testing of novel co-impregnated La$_{0.20}$Sr$_{0.25}$Ca$_{0.45}$TiO$_3$ anodes for commercial combined heat and power units

Robert Price[1] ⓘ | **Holger Bausinger**[2] | **Gino Longo**[2] | **Ueli Weissen**[2] | **Mark Cassidy**[1] | **Jan G. Grolig**[2] | **Andreas Mai**[2] | **John T. S. Irvine**[1]

[1]School of Chemistry, University of St Andrews, St Andrews, UK

[2]HEXIS AG, Winterthur, Switzerland

Correspondence
Robert Price, School of Chemistry, University of St Andrews, St Andrews, Fife, KY16 9ST, UK.
Email: rp63@st-andrews.ac.uk

Abstract

Over the past decade, the University of St Andrews and HEXIS AG have engaged in a highly successful collaborative project aiming to develop and upscale La$_{0.20}$Sr$_{0.25}$Ca$_{0.45}$TiO$_3$ (LSCT$_{A-}$) anode "backbone" microstructures, impregnated with Ce$_{0.80}$Gd$_{0.20}$O$_{1.90}$ (CG20) and metallic electrocatalysts, providing direct benefits in terms of performance and stability over the current state-of-the-art (SoA) Ni-based cermet solid oxide fuel cell (SOFC) anodes.

Here, we present a brief overview of previous work performed in this research project, including short-term, durability, and poison testing of small-scale (1 cm^2 area) SOFCs and upscaling to full-sized HEXIS SOFCs (100 cm^2 area) in short stacks. Subsequently, recent results from short stack testing of SOFCs containing LSCT$_{A-}$ anodes with a variety of metallic catalyst components (Fe, Mn, Ni, Pd, Pt, Rh, or Ru) will be presented, indicating that only SOFCs containing the Rh catalyst provide comparable degradation rates to the SoA Ni/cerium gadolinium oxide anode, as well as tolerance to harsh overload conditions (which is not exhibited by SoA anodes). Finally, results from full system testing (60 cells within a 1.5 kW electrical power output HEXIS Leonardo FC40A micro-combined heat and power unit), will be outlined, demonstrating the robust and durable nature of these novel oxide electrodes, in addition to their potential for commercialization.

KEYWORDS
anodes, micro-combined heat and power units, overload testing, solid oxide fuel cells, short stack

1 | INTRODUCTION

Solid oxide fuel cells (SOFCs) are efficient energy conversion devices which facilitate the electrochemical oxidation of fuel gases to provide a cleaner method of electricity generation to combustion of natural gas [1]. Due to the high operating temperatures required to allow oxide ion conduction in the solid-state electrolytes, the combination of high-quality heat and electrical power output makes SOFC technology desirable for combined heat and power

applications (in the 1–5 kW class), as well as for electricity generation at the MW scale [1, 2].

Typically, state-of-the-art (SoA) SOFC anode materials are composites of Ni metal and a ceramic, such as a stabilized zirconia (SZ) or cerium gadolinium oxide (CGO); also known as Ni-based cermets. Although the Ni-phase of these anodes provides good electronic conductivity and electrocatalytic activity for fuel oxidation, it can also lead to difficulties with redox cycling, coking, sulfur [3] and overload intolerance [4].

Over the past decade, research into an alternative SOFC anode material, $La_{0.20}Sr_{0.25}Ca_{0.45}TiO_3$ (LSCT$_{A-}$), as a replacement for the Ni-based cermet, has yielded extremely impressive results [4–12]. Employment of LSCT$_{A-}$ as an anode support microstructure eliminates the requirement to incorporate a structural Ni component and, when impregnated with electrocatalyst species, produces highly electrochemically active, nanostructured fuel electrodes. A comprehensive review of the history of development of these impregnated LSCT$_{A-}$ anodes has previously been published by the authors [4]; however, a brief summary is provided here.

Originally, preparation of SOFC electrodes through impregnation (and calcination) of catalyst nitrate precursors into pre-sintered electrode scaffold microstructures was performed by Craciun et al. [13], although many other research groups have since employed this method [14–23]. Initially, electrode "backbone" microstructures were formed from stabilised zirconia, with impregnated ceria and metallic catalysts [14–16], however, impregnation of perovskite materials (e.g., lanthanum strontium chromium manganese oxide) into the aforementioned "backbone" microstructures was also successfully achieved [17, 18]. Moreover, the use of perovskite materials as "backbone" microstructures into which electrocatalyst species can be impregnated, particularly perovskite titanate materials, has attracted much attention due to their mixed ionic and electronic conductivity, redox stability and processability [19–23]. LSCT$_{A-}$ is one such anode 'backbone' material which falls into this category and, when incorporated into an electrolyte-supported SOFC and impregnated with CeO_2 and Ni catalysts, gave rise to low area specific resistances (0.37 Ω cm^2) after 20 redox cycles and 250 h operation at 900°C in 92 % H_2/8 % H_2O [5]. In addition, Tiwari et al. reported that LSCT$_{A-}$ anodes (without impregnates) offer a low propensity for coking when operating in "dry" methane, while Ni et al. [6] and Lu et al. [7] presented promising initial performances when employing Ni, or CeO_2 and Ni, impregnated LSCT$_{A-}$ anodes in anode-supported SOFCs.

Verbraeken et al. made a highly promising initial attempt to integrate Ni and $Ce_{0.80}Gd_{0.20}O_{1.90}$ (CG20) co-impregnated LSCT$_{A-}$ anodes into the SOFCs of a full stack (60 cells) within the HEXIS Galileo 1000 N micro-combined heat and power (μ-CHP) system (1 kW electrical power output). However, it was identified that further optimization of the anode microstructure was required to increase effective electronic conductivity of the fuel electrode and prevent poor current distribution that led to high degradation in this stack [12]. Subsequently, re-optimization of this LSCT$_{A-}$ anode microstructure was successfully performed, giving rise to effective electronic conductivity values of 17 S cm^{-1} at 850°C and $p(O_2)$ 10^{-19} atm [8, 11, 24].

Testing of button SOFCs (1 cm^2 active area) containing these optimized LSCT$_{A-}$ anode microstructures impregnated with a variety of catalyst systems, including Ni/CG20, Pd/CG20, Pt/CG20, Rh/CG20 and Ru/CG20, gave rise to area specific resistances (ASR) of as low as 0.39 Ω cm^2 (at 0.8 V and 900°C in 3% H_2O/97% H_2) and confirmed that re-optimization of the anode microstructure was successful [8]. In particular, the promising performance of the Rh/CG20 co-impregnated LSCT$_{A-}$ anode warranted further examination under sulfur poisoning and durability testing conditions. After exposure to up to 8 ppm H_2S (mimicking a breakdown in the desulfurization unit of a μ-CHP system) this catalyst system exhbited a full recovery of performance after running at 850°C in non-humidified H_2 at 300 mA cm^{-2} for only 10 min [9], while durability testing of an analogous cell for over 3000 h, also at 850°C in non-humidified H_2 and 300 mA cm^{-2}, gave rise to a degradation rate of 1.9% kh^{-1} (18.5 mV kh^{-1}), which is impressive for this class of material [4].

These promising attempts to engineer a novel, robust anode material culminated in the production of a short stack of five full-sized HEXIS SOFCs containing optimized anodes (LSCT$_{A-}$ with CG20 and Rh impregnates). Successful upscaling of these anodes was carried out, giving rise to a short stack exhibiting a low degradation rate of 3.3 mV kh^{-1}, as well as stability towards redox cycling, thermoredox cycling, operation in sulfurized natural gas and overload exposure, offering direct benefits over the current SoA anode material [4].

In this report, we present results concerning further short stack testing of SOFCs containing a variety of LSCT$_{A-}$ anodes with CGO and metallic catalyst impregnates (Fe, Mn, Ni, Pd, Pt, Rh, and Ru), but in particular, we will discuss the testing of the Rh/CGO catalyst system for ~3000 h including overload or stress testing. Finally, data relating to upscaling of this technology to a 60 cell stack housed within a HEXIS Leonardo FC40A μ-CHP system, with a 1.5 kW electrical power output, will be presented, demonstrating the commercial potential of the materials developed over the past decade as a collaborative effort between the University of St Andrews and HEXIS AG.

TABLE 1 A summary of the average loading for each metallic catalyst employed in short stacks of full-sized HEXIS SOFCs.

Metallic catalyst	Average loading (mg/cm^2)	Stack number
Fe	0.014	1
Mn	0.014	1
Ni	0.017	2
Pd	0.030	2
Pt	0.034	3
Ru	0.025	3
Rh (Ref)	0.015	1 and 3

2 | EXPERIMENTAL

2.1 | Manufacture of full-sized HEXIS SOFC for short stack and full system testing

Full-sized HEXIS geometry SOFCs (~100 cm^2 active area) were produced according to experimental procedures outlined elsewhere [4]. Specific details concerning the ceramic processing, sintering and catalyst loadings of the SOFC are confidential, however, the SOFCs comprised 100 µm thick 6 mol.% scandia-stabilised-zirconia (6ScSZ, HEXIS), a lanthanum strontium manganite (LSM)-based cathode and an anode comprising LSCT$_{A-}$ with CGO and either: Fe, Mn, Ni, Pd, Pt, Rh, or Ru catalyst impregnates, which are introduced to the anode post-sintering through a nitrate precursor, wet impregnation method, as described previously [4, 8, 9, 14]. Average loadings of the metallic catalyst component are presented in Table 1.

2.2 | Short stack construction and testing

Construction of a series of short stacks, of five cells, containing the aforementioned titanate-based anodes, as well as a SoA HEXIS SOFC (with a Ni/CGO anode) or a SOFC with a Rh-impregnated titanate anode for reference, was carried out in order to assess the durability and tolerance of these novel SOFCs to harsh treatments. SOFCs were assembled into a stack along with Ni mesh current collectors (at the anode side) and metallic interconnect (MIC) plates, which facilitate current collection from the surface of the electrodes, in addition to allowing distribution of fuel and oxidant gases over the anode and cathode, respectively. The assembled short stacks were mounted in a "sealless" setup, in order to facilitate the establishment of a peripheral fuel combustion zone required to maintain the stack temperature. Schematics and information on the HEXIS stack concept and test rigs are reported elsewhere [25]. After installation of the stack and heating

to the operating temperature of 850°C, a flow of 4 g h^{-1} (which is equal to a heating value (H$_i$) of 50.8 W) per cell of natural gas (NG), reformed by Catalytic Partial Oxidation (CPOx), was fed to the anode compartments, whilst a flow rate of 200 g h^{-1} per cell of compressed air was supplied to the cathode compartments, to ensure the formation of the combustion zone at the edge of the stack. Under normal conditions, the stacks were subjected to galvanostatic operation at a stack current of 25 A, with regular voltage-current (VI) measurements, impedance spectroscopic analysis and exposure to overload cycling. However, for the short stacks containing LSCT$_{A-}$ anodes with differing metallic catalyst species, stack current was limited to 20 A or 15 A, depending on the initial operating voltages observed. Overload cycling of the cells involved increasing the stack current to ~40 A to ensure that a fuel utilisation >100% was achieved. Following each overload treatment, the stack current was returned to 25 A to resume normal operation. Overload, VI and alternating current (AC) impedance spectroscopic measurements were performed using a Zahner-Elektrik IM6 Impedance Spectrometer and a PP240 Potentiostat.

2.3 | Full system testing in HEXIS Leonardo FC40A µ-CHP unit

A series of 60 SOFCs, from the same production run, were also assembled into a full-sized stack for integration into a HEXIS Leonardo µ-CHP unit. After installation and commissioning, the system was operated at a constant stack voltage using an input of 4.5 kW (equivalent) NG, reformed by CPOx, yielding an electrical power output of 1.5 kW [26]. The system performance was monitored continuously for the first 330 h of operation.

3 | RESULTS AND DISCUSSION

3.1 | Short stack testing

3.1.1 | Variation of impregnated metallic catalyst component

Initially, three short stacks, each containing five SOFCs, were constructed in order to trial a variety of metallic catalyst species (Fe, Mn, Ni, Pd, Pt, Rh, and Ru); loadings of the metallic catalyst component are summarised in Table 1. Each stack contained one reference SOFC in the central position, to provide direct comparability to a SOFC, which has well-defined degradation characteristics.

Short stack 1 (Figure 1) comprised five SOFCs with the aforementioned LSCT$_{A-}$ and CGO components, two
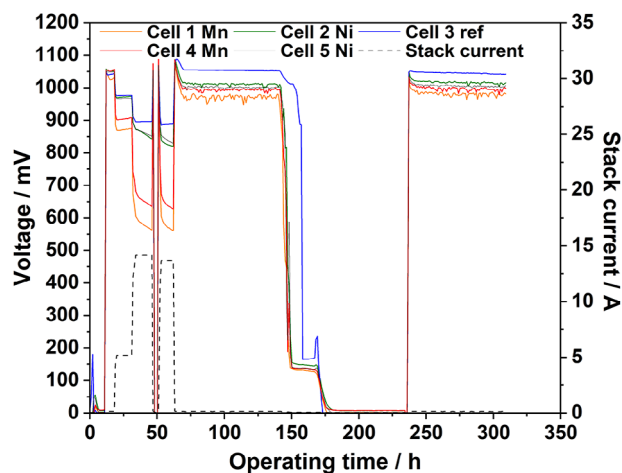
FIGURE 1 Test data for short stack 1, comprising SOFCs containing novel titanate-based anodes (two cells with a Ni catalyst, two cells with Mn a catalyst, and one cell with a Rh catalyst, for reference) operated for a total of 309 hours. The stack was operated at ~14 A between 20 and 62 hours, before returning to OCV and undergoing a thermoredox cycle between 141 and 237 hours.

FIGURE 2 Test data for short stack 2, comprising four SOFCs containing novel titanate-based anodes (two cells with a Fe catalyst and two cells with a Pd catalyst), and one SoA HEXIS SOFC (for reference) operated for a total of 240 hours. Galvanostatic operation of the stack at 20 A was carried out between 33 and 54 hours, as well as at 21 A for a brief period around 98 hours.

containing a Mn catalyst, two containing a Ni catalyst and one reference SOFC containing a Rh catalyst. Following heat-up and the commissioning period at 5 A (20–31 hours), the stack current was increased to 14.2 A. Typically, short stacks are operated at 25 A stack current, however, as shown by the cell voltages in Figure 1, the SOFCs with the Mn-containing anodes degrade severely (by 44 mV and 46 mV for cells 1 and 4, respectively, between 34 and 46 hours) at a much lower operational current. The SOFCs with the Ni-containing anodes also show high degradation (29 mV and 20 mV for cells 2 and 5, respectively, between 34 and 46 hours) in comparison to the reference SOFC, which exhibits a relatively stable operating voltage, as expected. The reference cell voltage does appear to degrade slightly after the current is interrupted and subsequently restored to 13.7 A between 46 and 54 hours, although this is likely due to the fact that the reference SOFC compensates for the poor performance of the remaining SOFCs in the short stack. After returning to open circuit voltage (OCV) at ~62 hours, all SOFCs except for the reference cell show unstable voltages and so the stack was subjected to a thermoredox cycle in order to determine whether this might improve contact between the Ni mesh current collector at the anode surface. No improvement was observed after this treatment therefore the test was terminated.

Figure 2 displays the performance of short stack 2, comprising two SOFCs containing a Fe catalyst, two SOFCs containing a Pd catalyst and one SoA HEXIS SOFC (with a Ni/CGO anode) for reference. After heating and commissioning the stack at ~21 hours with 5 A stack current, a brief increase to 24.5 A (close to standard operating cur-
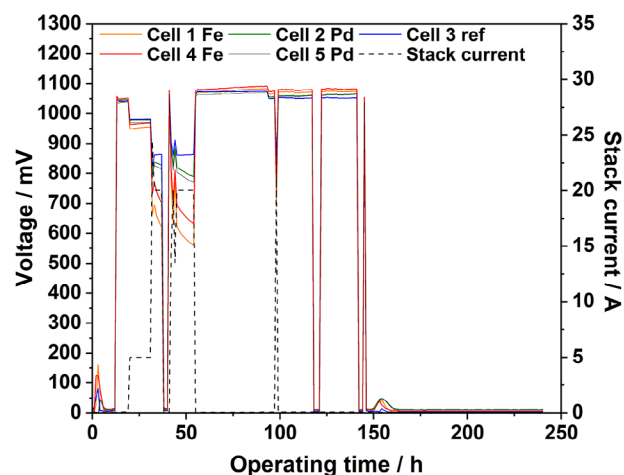
rent) revealed critically low operating voltages of the Fe-containing cells. Therefore, the stack current was reduced to 20 A to provide some useful information on degradation of the cells. In similarity to the Mn-containing SOFCs displayed in Figure 1, the Fe-containing cells degraded sharply, by 135 mV and 138 mV for cells 1 and 4, respectively, between 33 and 54 hours, during which time a redox cycle was also performed. Although the degradation of the two Pd-containing SOFCs was lower (49 mV and 57 mV for cells 2 and 5, respectively, between 33 and 54 hours, in comparison to the Fe-containing SOFCs, it is still considered to be unacceptably high relative to the HEXIS SoA and novel SOFCs containing LSCT$_{A-}$ anodes with CGO and Rh catalysts. As a result, this stack test was also terminated after 240 hours.

Finally, short stack 3 (Figure 3) included two SOFCs with a Pt catalyst, two SOFCs with a Ru catalyst, and one reference SOFC with a Rh catalyst. After heating the stack and commissioning at 5 A over the first 22 hours, the stack current was increased to 20 A, with all SOFCs exhibiting significantly higher operating voltages than observed for the short stacks in Figures 1 and 2. The voltages of the Ru-containing cells were lower than the Pt or Rh-containing counterparts, however, after a redox cycle was carried out between 105 and 110 hours, these values improved to be almost identical (865 – 868 mV) to the Rh-containing SOFC (866 mV). This provided some initial promise that a more abundant and less expensive platinum group metal (PGM) may be able to replace the Rh electrocatalyst. Operating voltages were monitored at 20 A until 207 hours when it was increased to 25 A stack current for normal
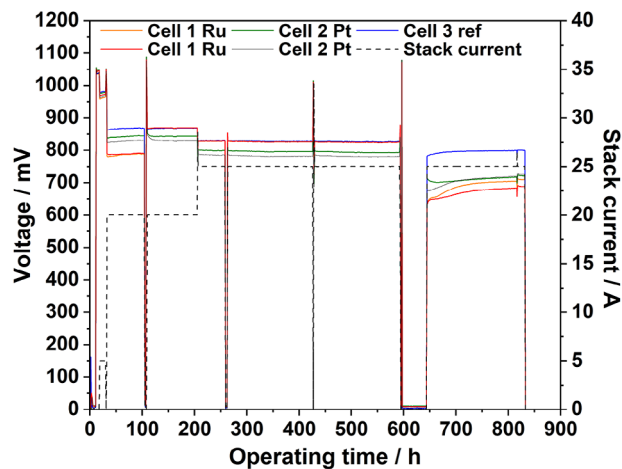
FIGURE 3 Test data for short stack 3, comprising SOFCs containing novel titanate-based anodes (two cells with a Ru catalyst, two cells with a Pt catalyst, and one cell with a Rh catalyst, for reference) operated for 833 hours. The short stack was operated at 20 A between 22 and 207 hours, before the current was increased to 25 A until 593 hours. Subsequently, the stack was exposed to an overload or stress test until 644 hours, with galvanostatic operation resuming (at 25 A) until the end of the operational period.

operation. Once again, the Rh and Ru-containing cells showed almost identical operating voltages (829-830 mV) with good stability over a period of 386 hours, while the Pt-containing SOFCs exhibited slightly lower voltages (801 mV and 788 mV for cells 2 and 5, respectively) with higher degradation. Subsequently, at 593 hours an overload test was performed until 644 hours by increasing the stack current to 40 A using the external AC impedance spectrometer/potentiostat equipment; hence the data for the current was not captured during this period. Following reinstatement of normal operating conditions at 645 hours, the operating voltages of all SOFC gradually recover, but the Rh-containing reference cell exhibited the highest voltage, followed by the Pt-containing cells and Ru-containing cells. After a small interruption of current at 818 hours, the operating voltages of all SOFC began to degrade, except for the Rh-containing reference cell, prior to shutdown of the stack at 833 hours.

Overall, this series of short stack experiments has demonstrated that the transition metal catalysts, Fe and Mn, give rise to unacceptably high degradation in SOFCs at industrially relevant scales. The Ni catalyst exhibits lower degradation in comparison to its Fe and Mn counterparts, instead offering similar degradation trends to the Pd catalyst. The remaining PGM metallic electrocatalysts (Pt, Rh, Ru) offer the highest operating voltage stability at a short stack scale; however, only the Rh catalyst can provide a high level of tolerance toward overload conditions (at a low
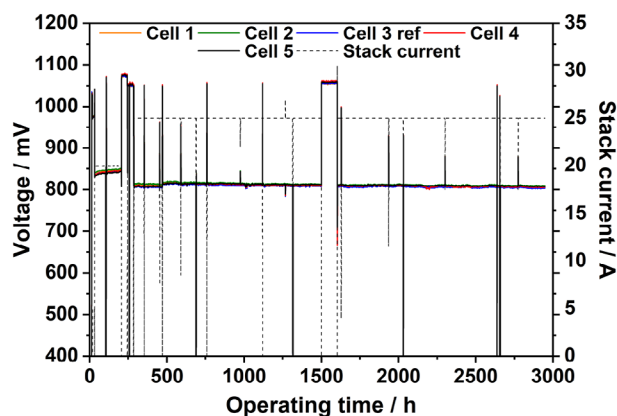

FIGURE 4 Long-term test data for a short stack comprising one SoA HEXIS SOFC and four SOFCs containing novel titanate-based anodes with CGO and Rh impregnates operated at a stack current of 25 A for 2949 hours.

catalyst loading of 0.015 mg cm^{-2}), which is a crucial aspect for the HEXIS system.

3.1.2 | Durability and overload testing of SOFCs with Rh-impregnated anodes

Based upon the information obtained regarding the catalyst optimisation experiments described in the previous section, further durability testing of SOFCs containing the novel titanate-based anodes with CGO and Rh electrocatalysts was carried out. Figure 4 displays the long-term test data for a short stack containing 5 SOFCs; 1 reference (SoA HEXIS) SOFC positioned at the centre of the stack, and 4 SOFCs containing the novel, titanate-based anodes with CGO and Rh impregnates positioned at the ends of the stack. All cell voltages are similar and this narrow dispersion demonstrates a clear improvement over the preceding generation of titanate cells tested at short stack scale in the authors' previous work [4]. During this operational period, the short stack was allowed to run continuously, with only short periods offline required to perform AC impedance spectroscopic analysis and VI measurements.

Figure 5 illustrates the evolution of area specific resistance (ASR) as a function of operational time. During the first 490 hours of operation, a series of corrections to the air flow rate were performed in order to counteract the effect of a crack in the manifolding to the cathode chambers of the SOFC stack, explaining the dramatic, step-wise reductions in ASR within this time-frame. After normal operation resumed at 490 hours, the ASR of all cells degraded at a similar rate, although the ASR of cell 4 was slightly higher than for the rest of the stack. The average degradation rate for the four SOFCs containing impregnated LSCT$_{A-}$ anodes was calculated to be
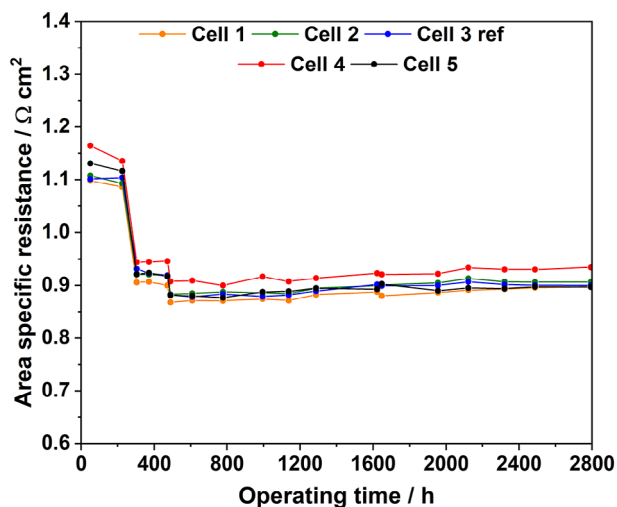
FIGURE 5 Plot of ASR versus operational time for the short stack containing four SOFCs with novel titanate-based anodes with CGO and Rh electrocatalysts and one SoA HEXIS SOFC.

10.3 mΩ cm^2 kh^{-1}, compared to 7.3 mΩ cm^2 kh^{-1} for the SoA HEXIS reference SOFC, during this time period. The average voltage degradation for the SOFCs containing impregnated LSCT$_{A-}$ anodes was calculated to be 3.7 mV kh^{-1} (0.46% kh^{-1}), compared to 3.8 mV kh^{-1} (0.47% kh^{-1}) for the reference cell, over this initial period. This shows that the SOFCs containing the novel anodes investigated over the past decade do in fact provide extremely similar degradation behaviour and performance to the SoA HEXIS Ni/CGO-based anodes. Furthermore, Figure 6 provides a comparison of VI curves collected after the corrections to stack airflow had been made at 590 hours (a) and after the initial period of operation at 25 A stack current concluded at 2775 hours (b). Performance over this operational period does not appear to have degraded significantly and cells 3 and 4 both show improvements in the higher-current region of the VI curve.

Benefits of these novel anodes identified in previous research include their high stability toward redox and thermoredox cycling, as well as their ability to operate in sulfur-laden NG (e.g., during a breakdown of desulfurization unit) [4]. Following the initial 2949 hours of testing, the robustness of the stack to an additional harsh treatment was investigated. Here, sudden fuel supply shutdowns (during which current may still be drawn from the stack) were mimicked in order to assess the ability of the stack to tolerate overload conditions. Figure 7a shows that three periods of overload exposure were carried out between 3115–3118 hours, 3134–3142 hours and 3159–3184 hours. In between each overload cycle, normal operation at 25 A stack current resumed. In each cycle, as the stack current rises to almost 40 A, due to the increased fuel utilization, the operating voltage of all SOFCs decrease
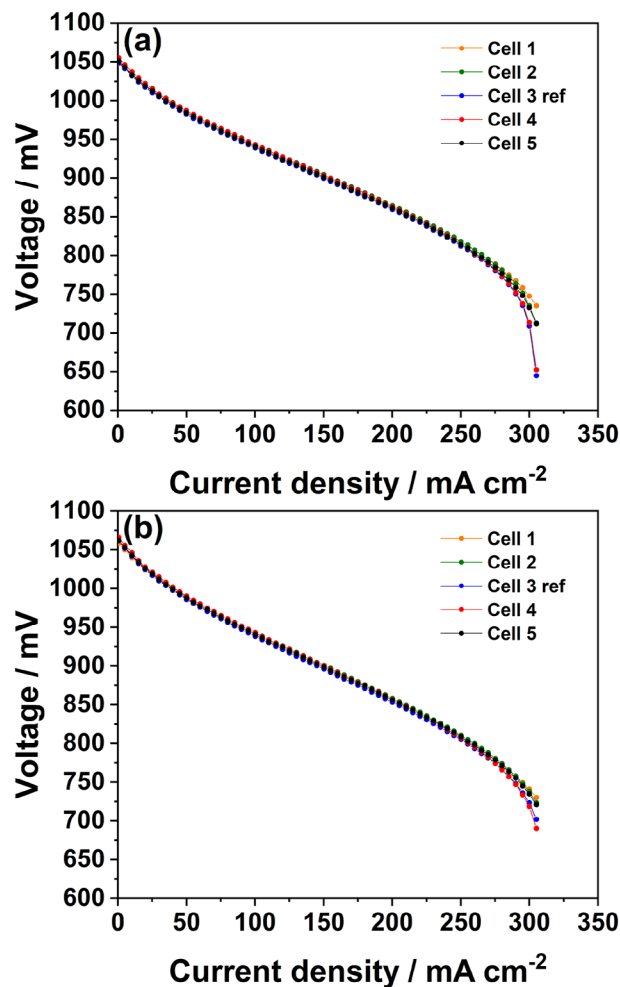

FIGURE 6 VI curves for the short stack (containing four SOFCs with novel titanate-based anodes with CGO and Rh electrocatalysts and one SoA HEXIS SOFC) collected after (a) 590 hours and (b) 2775 hours of operation.

and become negative, establishing the so-called overload conditions. After this initial rapid drop in operating voltage, cells 1 and 2 respond very well to overload exposure, exhibiting a stabilization and, ultimately, an increase in voltage as a function of time. In contrast, cells 4 and 5 continue to degrade throughout the exposure period. As expected, the reference cell displays the largest initial voltage drop (due to poor overload tolerance of the SoA Ni/CGO anodes), although a slight stabilization and recovery of voltage is observed during the second and third overload cycles.

Significantly, following the conclusion of the third and final overload exposure, the stack was operated at 25 A under normal conditions. It can be seen that the operating voltages of cells 1 and 2 recover quickly to 776 mV and 768 mV, respectively, which are quite similar to the operating voltages noted during the first 2949 hours of operation (806 mV and 810 mV, respectively). The operating
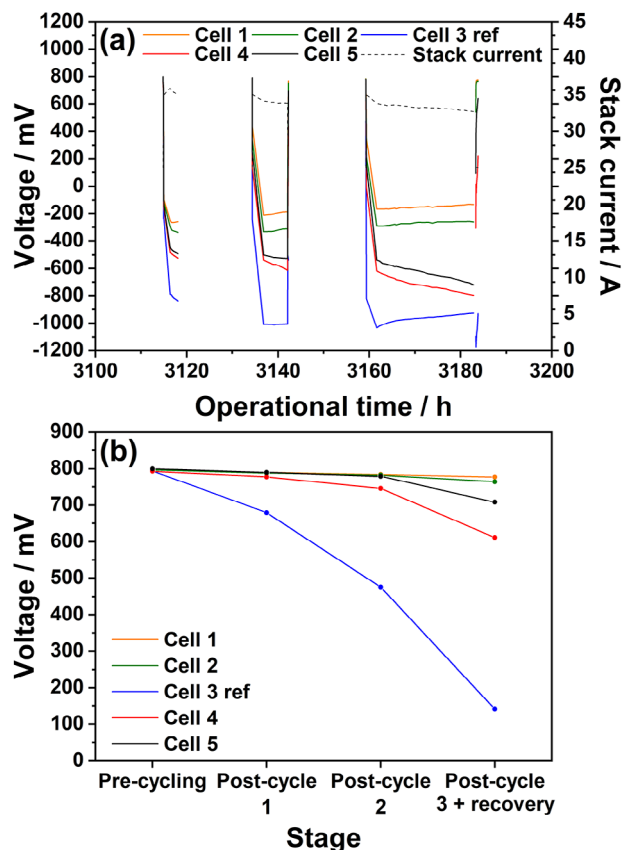
FIGURE 7 (a) Plot of cell voltage and stack current versus time, during a period of overload testing, performed after the initial 2949 hours of operation of the short stack (containing four SOFCs with novel titanate-based anodes with CGO and Rh electrocatalysts and one SoA HEXIS SOFC) and (b) a plot illustrating the evolution of cell operating voltage as a function of overload cycling.

voltages of cells 4 and 5 (262 mV and 651 mV, respectively) are lower than those of cells 1 and 2; however, the rapid increase of the voltage indicates that the recovery of these cells is incomplete. Similarly, the voltage of the reference cell also appears to be recovering after the third overload cycle; however, this is occurring in a much slower manner. Figure 7b illustrates the evolution of operating voltages (in the presence of CPOx reformed NG and under 25 A stack current) of each cell before the overload cycling period, after overload cycles 1 and 2 and, finally, after a recovery period of ~168 hours (following the third overload cycle) under standard operating conditions. Although the operating voltages of cells 1 and 2 remain stable during this period, those of cell 4 and 5 exhibit further recoveries to 611 mV and 708 mV, respectively. Despite the fact that all of the SOFCs containing the novel titanate-based anodes exhibit a slight degradation in operating voltage after three intense periods of overload cycling, the reference SOFC is no longer functional and can only manage to operate at 142 mV under standard conditions. This evi-

dences the greatly superior stability of the titanate-based anodes under harsh conditions, in comparison to the SoA anode, which is not able to operate or recover from exposure to the same treatments. However, one must also take into account that the gas distribution within a stack has a statistical variation, therefore, the reference cell might also have received slightly less gas than the others and so was exposed to a harsher overload than the others. The deviation of the VI curves of cells 3 and 4 in the higher-current (concentration polarization) region of Figure 6a point toward effects of these mass transport limitations. Consequently, more overload tests are planned to evidence the improved overload capability of the titanate-based cells.

AC impedance spectroscopy of each SOFC within the short stack was performed at various stages throughout operation in order to understand cell degradation as a function of time and overload cycling. Figure 8 displays AC impedance spectra collected at (a) 696 hours, (b) 2040 hours, (c) 3120 hours (before overload cycling) and (d) 3288 hours (after overload cycling). The AC impedance spectra collected during short stack testing typically comprise three discernible processes: (i) a high frequency anode-related process [4, 8–10], (ii) a mid-frequency cathode-related process [4, 8–10, 27] and (iii) a dominant low-frequency gas conversion process that is characteristic of stack scale testing, due to the high fuel utilization employed. This masks the mid to low-frequency features that can usually be identified during button cell (1 cm^2) testing [12]. The anode and cathode-related processes exhibit good stability during the first 3120 hours of testing (Figures 8a–c), with the only notable increase in ASR being contributed by the degradation of conductivity within the 6ScSZ electrolyte [28] and the growth of oxide layers on the metallic interconnects [29], increasing the ohmic resistance (R_s) of the SOFCs; both well-known and expected degradation mechanisms.

After exposure of the stack to three overload cycles, the spectra of cells 1 and 2 indicate that the anode and cathode-related processes still remain unchanged, although R_s continued to degrade. By comparison, cells 4 and 5, which also contain the novel titanate-based anodes, displayed large increases in R_s (0.346 and 0.197 Ω cm^2, respectively), which may be attributed to worsening of current collection at the surface of the anode or delamination at the anode-electrolyte interface. This is corroborated by the increase in anode polarization resistance, although it should be mentioned that worsening of current collection at the electrodes can also proportionally increase the polarization resistance of cells, explaining the slight increases in resistances of the cathode and gas conversion processes. However, considering the spectrum of the SoA HEXIS SOFC, it is possible to see that a large increase in R_s is
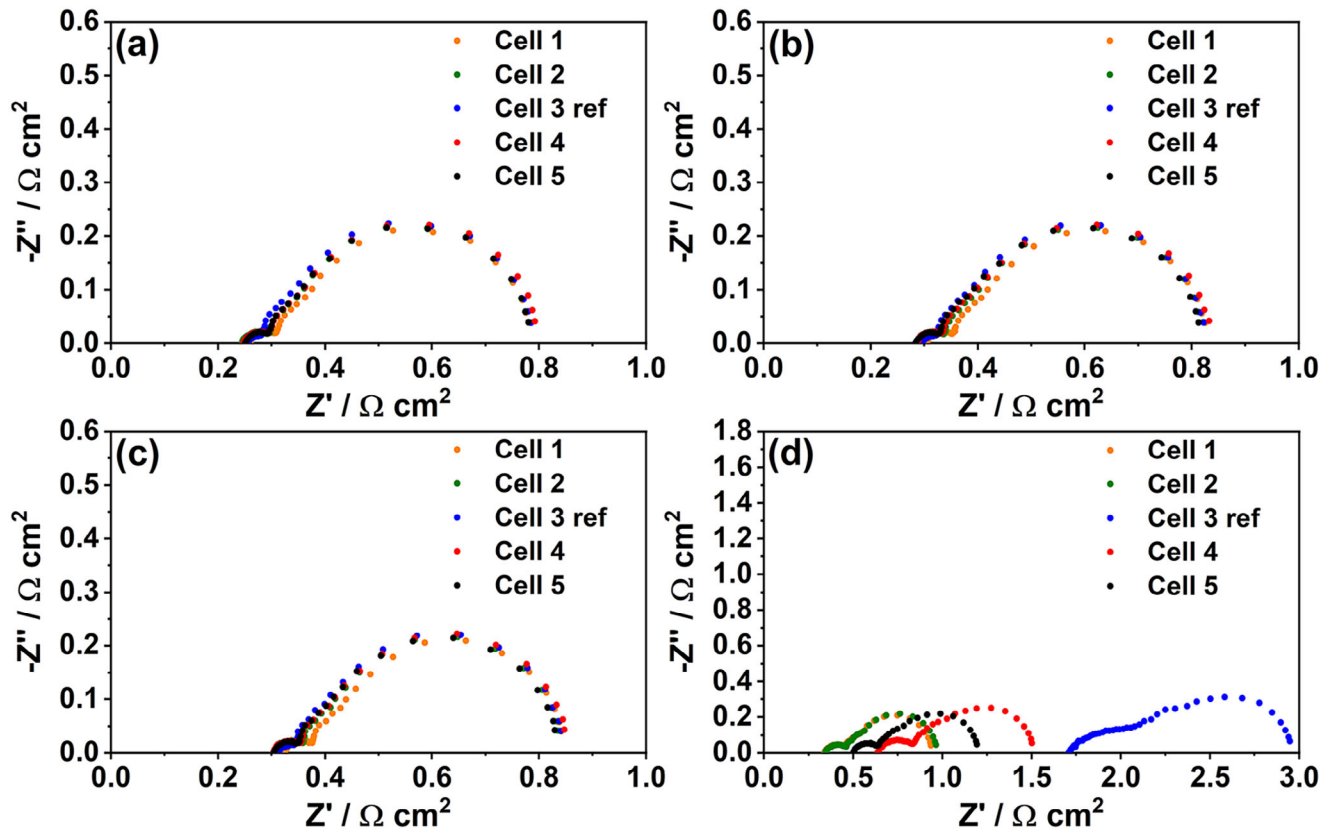
FIGURE 8 Complex plane AC impedance spectra for each SOFC within the short stack (containing four SOFCs with novel titanate-based anodes with CGO and Rh electrocatalysts and one SoA HEXIS SOFC) collected at 15 A after (a) 696 hours, (b) 2040 hours, (c) 3120 hours (before overload cycling), and (d) 3288 hours (after overload cycling).

responsible for the severe degradation of this cell in addition to an increase in the polarization resistance of the anode-related processes. As also shown by cells 4 and 5, proportional increases in the cathode and gas diffusion processes are related to the worsening of current collection and increased R_s. Overall, the impedance spectra provide insights into the comparative stability of the novel titanate-based to the SoA Ni/CGO cermet anodes under overload conditions.

3.2 | Full system testing in the HEXIS Leonardo FC40A μ-CHP unit

In order to provide proof-of-concept for the potential of these anodes within a commercial product, a further upscaling step of the novel titanate-based SOFC anode technology, to a full 60 cell stack within a HEXIS Leonardo FC40A μ-CHP system, was undertaken. Figure 9 displays the system test data collected during the first 330 hours of operation. Following the commissioning period (~70 hours), the power output reaches the nominal value of 1.5 kW (electric) at a constant gas input of 4.0 kW (equivalent), an operating temperature of 850°C and a stack

voltage of 42 V, showing an improvement over the original system test using this class of anode in the HEXIS Galileo 1000 N μ-CHP unit performed by Verbraeken et al. [12]. Unfortunately, due to an issue relating to gas flow to the single, bottom-most cell of the stack, the gas input was increased to 4.5 kW (equivalent), to compensate for some of the degradation, whilst the operating voltage was lowered stepwise to 36 V, consequently reducing the power output to ~1.35 kW, in order to protect the stack. A
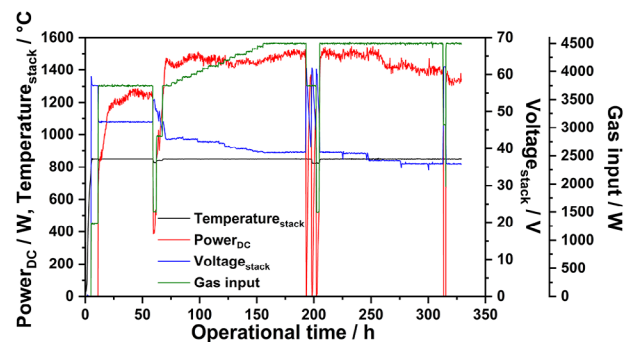

FIGURE 9 Test data for a 60 cell stack of SOFCs containing the novel titanate-base anodes, tested within a HEXIS Leonardo FC40A μ-CHP unit for 330 hours.

shutdown is currently in progress to rectify the situation and normal operation is expected to resume in the near future to continue testing these novel titanate-based anodes at an industrially relevant scale. Despite the temporary shutdown of this system after ∼300 hours, the ease with which the nominal power output of the μ-CHP system can be achieved is a promising sign for the potential of these novel titanate-based anodes. In addition, the large temperature gradient across the stack, observed during the original Galileo system test involving these materials, no longer appears to be an issue and all cells (with the exception of the bottom-most cell) within the stack are noted to be operating within the voltage and temperature ranges expected for a standard HEXIS stack.

4 | CONCLUSIONS

As a result of a successful academic-industrial collaboration between the University of St Andrews and HEXIS AG, a fourth-generation short stack of SOFCs containing novel titanate-based anodes with CGO and Rh impregnates, has been tested for over 3000 hours, exhibiting degradation rates similar to those expected for the standard HEXIS SOFC containing Ni/CGO anodes. In addition to the previously demonstrated redox and thermoredox cycling stability, and tolerance to operation in sulfur-laden NG, by the third-generation short stack, it has been shown that these anodes also provide increased stability towards overload cycling (continued drawing of current from the stack in the event of a fuel supply failure). Short stack scale evaluation of SOFCs containing different metallic catalyst components (Fe, Mn, Ni, Pd, Pt, Rh, and Ru) indicated that only the Rh catalyst could provide similar stability to degradation as the SoA HEXIS SOFC and tolerance to overload or stress testing, validating the use of LSCT$_{A-}$ anode with CGO and Rh impregnates. This provides several benefits over the SoA anode material and could allow simplification and cost-reduction of future μ-CHP systems. Furthermore, upscaling of this anode technology to a full 60 cell stack, integrated into a HEXIS Leonardo FC40A μ-CHP system, has been successful, demonstrating the ability to reach the nominal 1.5 kW (electrical) power output with ease. Despite encountering an issue with the bottom-most cell within the stack, warranting a shutdown to rectify this situation, this shows a direct improvement in performance over the previous system test carried out in the HEXIS Galileo 1000 N μ-CHP system (1 kW electrical power output).

ORCID

Robert Price https://orcid.org/0000-0003-2897-6948

REFERENCES

1. P. Holtappels, U. Stimming, in *Handbook of Fuel Cells – Fundamentals, Technology and Applications*, (Eds.: W. Vielstich, A. Lamm, H. A. Gasteiger), John Wiley & Sons, Chichester, UK, **2003**.
2. J. G. Grolig, H. Bausinger, V. Sarda, C. Meier, A. Mai, *ECS Trans.* **2021**, *103*, 275.
3. C. Sun, U. Stimming, *J. Power Sources* **2007**, *171*, 247.
4. R. Price, M. Cassidy, J. G. Grolig, G. Longo, U. Weissen, A. Mai, J. T. S. Irvine, *Adv. Energy Mater.* **2021**, *11*, 2003951.
5. M. C. Verbraeken, B. Iwanschitz, A. Mai, J. T. S. Irvine, *J. Electrochem. Soc.* **2012**, *159*, F757.
6. C. Ni, L. Lu, D. N. Miller, M. Cassidy, J. T. S. Irvine, *J. Mater. Chem. A* **2018**, *6*, 5398.
7. L. Lu, C. Ni, M. Cassidy, J. T. S. Irvine, *J. Mater. Chem. A* **2016**, *4*, 11708.
8. R. Price, M. Cassidy, J. G. Grolig, A. Mai, J. T. S. Irvine, *J. Electrochem. Soc.* **2019**, *166*, F343.
9. R. Price, J. G. Grolig, A. Mai, J. T. S. Irvine, *Solid State Ionics* **2020**, *347*, 115254.
10. R. Price, U. Weissen, J. G. Grolig, M. Cassidy, A. Mai, J. T. S. Irvine, *J. Mater. Chem. A* **2021**, *9*, 10404.
11. R. Price, M. Cassidy, J. A. Schuler, A. Mai, J. T. S. Irvine, *ECS Trans.* **2015**, *68*, 1499.
12. M. C. Verbraeken, B. Iwanschitz, E. Stefan, M. Cassidy, A. Mai, J. T. S. Irvine, *Fuel Cells* **2015**, *15*, 682.
13. R. Craciun, S. Park, R. J. Gorte, J. M. Vohs, C. Wang, W. L. Worrell, *J. Electrochem. Soc.* **1999**, *146*, 4019.
14. P. A. Connor, X. Yue, C. D. Savaniu, R. Price, G. Triantafyllou, M. Cassidy, G. Kerherve, D. J. Payne, R. C. Maher, L. F. Cohen, R. I. Tomov, B. A. Glowacki, R. V. Kumar, J. T. S. Irvine, *Adv. Energy Mater.* **2018**, *8*, 1800120.
15. N. Christiansen, S. Primdahl, M. Wandel, S. Ramousse, A. Hagen, *ECS Trans.* **2013**, *57*, 43
16. H. He, R. J. Gorte, J. M. Vohs, *Electrochem. Solid-State Lett.* **2005**, *8*, A279.
17. G. Kim, G. Corre, J. T. S. Irvine, J. M. Vohs, R. J. Gorte, *Electrochem. Solid-State Lett.* **2008**, *11*, B16.
18. G. Corre, G. Kim, M. Cassidy, J. M. Vohs, R. J. Gorte, J. T. S. Irvine, *Chem. Mater.* **2009**, *21*, 1077.
19. G. Kim, M. D. Gross, W. Wang, J. M. Vohs, R. J. Gorte, *J. Electrochem. Soc.* **2008**, *155*, B360.
20. J. Nielsen, Å. H. Persson, B. R. Sudireddy, J. T. S. Irvine, K. Thydén, *J. Power Sources* **2017**, *372*, 99.
21. T. Ramos, S. Veltzé, B. R. Sudireddy, P. Holtappels, *ECS Electrochem. Lett.* **2014**, *3*, F5.
22. S. Veltzé, B. R. Sudireddy, P. S. Jørgensen, W. Zhang, L. T. Kuhn, P. Holtappels, T. Ramos, *ECS Trans.* **2013**, *57*, 743.

23. C. D. Savaniu, D. N. Miller, J. T. S. Irvine, *J. Am. Ceram. Soc.* **2013**, *96*, 1718

24. R. Price, M. Cassidy, J. A. Schuler, A. Mai, J. T. S. Irvine, *ECS Trans.* **2017**, *78*, 1385.

25. A. Mai, B. Iwanschitz, U. Weissen, R. Denzler, D. Haberstock, V. Nerlich, J. Sfeir, A. Schuler. *ECS Trans.* **2009**, *25*, 149.

26. A. Mai, J. G. Grolig, M. Dold, F. Vandercruysse, R. Denzler, B. Schindler, A. Schuler, *ECS Trans.* **2019**, *91*, 63.

27. M. J. Jørgensen, M. Mogensen, *J. Electrochem. Soc.* **2001**, *148*, A433.

28. M. R. Terner, J. A. Schuler, A. Mai, D. Penner, *Solid State Ionics* **2014**, *263*, 180.

29. J. G. Grolig, G. Longo, A. Mai, *ECS Trans.* **2019**, *91*, 2181.